Electrochemical-Impedance-Spectra Modelling by the Finite Element Method: Time/Frequency Considerations

ECS Transactions, 94 (1) 251-257 (2019)
10.1149/09401.0251ecst ©The Electrochemical Society

Electrochemical-Impedance-Spectra Modelling by the Finite Element Method: Time/Frequency Considerations

R. Mayen-Mondragon, R. Montoya-Lopez and J. Genesca-Llongueras

Polo Universitario de Tecnología Avanzada, Facultad de Química, Universidad Nacional Autónoma de México, Apodaca, Nuevo León, 66629, México

A one-dimensional computational-model was developed to simulate the electrochemical impedance response of two simultaneous generic-electrochemical-reactions taking place within an electrochemical cell with two opposite electrodes. The charge transfer process at the electrode/electrolyte interface (single step reaction) was described by the Butler-Volmer equation. The mass transfer process considered only diffusive components. Discussion of the graphical output was performed in terms of the lead/lag between current response and voltage input. The lead/lag between the latter and the species concentration was also discussed. Correlation of the frequency domain signal to the recovered time-domain profiles was performed. The model reliability was assessed. The model main purpose is to aid shifting from the study of electrochemical systems in the time domain to the frequency domain.

Introduction

Electrochemical Impedance Spectroscopy has been widely implemented to the study of electrochemical systems (1-5). The technique has the capacity to resolve individual physical processes according to the rate at which they proceed. Thus, it can many times be used to identify the reaction rate-limiting step. Such information can help develop strategies to improve the operation of an electrochemical system. Analysis of the impedance signal requires firstly to define an equivalent circuit whose electrical response matches the electrochemical-system impedance response. The type and arrangement of electrical elements therein can many times be guessed from the impedance spectrum morphology and the most relevant mechanisms expected to participate in the reaction. Experience is in such case of great aid to swiftly assemble a suitable circuit. The experience-gathering process can be advantageously accelerated by modeling the impedance response of electrochemical cells. Models of simple systems can be initially developed. Additional elements can then be step-wise integrated to understand its individual effect on the impedance spectra morphology. In each case, recovering and analyzing the time profile of the frequency-domain signals is essential to state the computational models reliability. Such analysis is, however, less straightforward than that of direct current (DC) systems. This is due to the frequency-dependent lead/lag that may exist between voltage input and current response. The direction of movement of reacting species and the transfer of charge at the electrode/electrolyte interface may also lag the voltage input. All such details can be derived from the signal phase which,

together with the signal amplitude, is related to the real and imaginary components of the impedance.

The present work describes some of our current advances in developing simple electrochemical-impedance-models by the finite element method using the software FlexPDE v. 6.23. Our previous experiences with the software can be found in the literature (6, 7). This time, however, the major challenge was the implementation of complex differential equations, as well as the transformation of the Butler-Volmer equation describing the transfer of charge at the electrode/electrolyte interface. Emphasis is made on analyzing the graphical output as a classroom tool for undergraduate and graduate students.

Model

The one-dimensional computational model was implemented as a script and solved by the finite element method with the FlexPDE v.6.23 software. The domain length was $d = 6\text{x}10^{-4}$ m (micrometric electrochemical cell). A generic electrochemical reaction took place at each domain end (Equation 1):

$$O_k + e^- \leftrightarrow R_k \qquad [1]$$

A complex diffusion equation (Equation 2) was set for each of the four participating species:

$$i\omega C_k + \nabla \cdot \left(-D_k \nabla C_k\right) = 0 \qquad [2]$$

where i is the imaginary unit, ω is the angular frequency of the alternating voltage signal (input), D_k is the diffusion coefficient of species k and C_k is the complex concentration of species k. The boundary condition at the electrodes surface (for the species reacting thereat) is:

$$-D_k \nabla C_k = \frac{J_R}{nF} \qquad [3]$$

where n is the number of transferred electrons, F is the Faraday constant (96,486 C/mol e) and J_R is the complex current density for the heterogeneous electrochemical reaction (Equation 4):

$$J_R = nFk^0\left(\left[C_{R,0} + C_R^*\right]\exp\left[\frac{(n-\alpha_c)F\eta}{RT}\right] - \left[C_{O,0} + C_O^*\right]\exp\left[\frac{-\alpha_c F\eta}{RT}\right]\right) \qquad [4]$$

where k^0 is the standard reaction rate constant, α_c is the cathodic charge transfer coefficient, η is the applied complex overpotential, $C_{R,0}$ and $C_{O,0}$ are, respectively, the complex concentration of the reduced and oxidized species at the electrode surface, C^*_k is the concentration of species k in the solution bulk, R is the universal gas constant and T is the absolute temperature.

The non-faradaic current density (due to the double layer capacitance) was added to Equation 4, and led to the total current density:

$$J = J_R + iC_{dl}\omega\eta \quad [5]$$

where C_{dl} is the electrical double layer capacity.

The impedance amplitude was calculated from the complex-voltage to complex-current ratio. The impedance phase was calculated applying the CARG FlexPDE-function which determines the argument or angular component of a complex quantity.

The model was solved for identical reactions considering $C^*_k = 1$ mol/m^3, $D_k = 1\text{x}10^{-10}$ m^2/s, $\alpha_c = 0.5$, $k^0 = 1\text{x}10^{-5}$ m/s, $C_{dl} = 0.2$ F/m^2, $n = 1$ and $T = 298.15$ K. The input potential amplitude at each electrode was $5\text{x}10^{-3}$ V. The signal frequency (f) was scanned from $1\text{x}10^{-2}$ Hz to $1\text{x}10^{4}$ Hz.

Results and Discussion

The continuous line in Figure 1 presents the typical Nyquist plot for one of the modelled electrochemical reactions. A long 45° diffusion tail can be observed at low frequencies. On the other side, in the medium and high frequency range, the typical capacitive semicircle is dominant (8). The semicircle arises from the combination of the charge transfer process at the electrode/electrolyte interface and the electrical double layer charge/discharge mechanism. A similar impedance spectra was derived using the Comsol Multiphysics Electrochemistry Module (dotted line in Fig 1). For the same model parameters, a good match was found between both.

Figure 2 presents the Bode plot associated to the Nyquist representation in Figure 1. The impedance phase (Fig. 2b) is close to -45° at low frequencies, as expected for the spectrum region where mass transport controls the reaction rate. At higher frequencies, the impedance phase approaches 0° and then shifts towards -90° (the latter according to the current lag promoted by the double layer capacitor). The impedance amplitude at the region where the phase ≈ 0° corresponds to the reaction charge-transfer-resistance (R_{ct}). According to the proposed reaction mechanism, the impedance data was fit (using the EIS Spectrum Analyzer software) to a Randles-type 3-element equivalent-circuit. The circuit considers null electrolyte resistance and a double-layer-capacitance in parallel with a charge-transfer-resistance and Warburg-diffusion element (W). The fitting session results are $C_{dl} = 0.201$, $R_{ct} = 0.026$ and W = 0.0385 with very good fit statistics. k^0 can be derived from R_{ct} according to the following equation (9):

$$k^0 = \frac{RT}{n^2 F^2 A\left(C_O^*\right)^{1-\alpha_c}\left(C_R^*\right)^{\alpha_c} R_{ct}} = 1.02x10^{-5} \quad [6]$$

D_k can be derived from (9):

$$D_k = \left(\frac{RT}{\sigma F^2 A\sqrt{2}}\left(\frac{2}{C_k^*}\right)\right)^2 = 9.6x10^{-11} \quad [7]$$

It can be observed that k^0 and D_k are quite similar to those used to feed the computational model. The largest difference (around 5%) was found for D_k and stems from the fitting procedure error and the maximum allowed error set for the finite element calculations. The previous results prove the developed-computational-model reliability.

Figure 3a shows the potential time-profile recovered from the complex-potential signal for a frequency $f = 1x10^{-2}$ Hz (mass-transport-controlled region). As the voltage is the input signal, it has the expected wave shape within one full cycle of 100 s. At that frequency the impedance phase shift is about -40° indicating the current leads the voltage for about 1/9 cycle, i.e. around 11 s, as can be shown in Figure 3b. Moreover, the voltage/current behavior goes in accordance with the proposed sign convention: positive oxidation currents for positive electrode overpotentials.

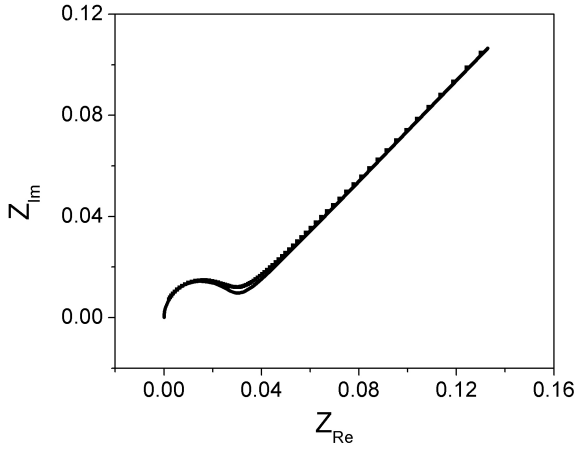

Figure 1. Nyquist plot of the modelled electrochemical reaction with $C^*_k = 1$ mol/m^3, $D_k = 1x10^{-10}$ m^2/s, $\alpha_c = 0.5$, $k^0 = 1x10^{-5}$ m/s, $C_{dl} = 0.2$ F/m^2, $n = 1$, $T = 298.15$ K, and $d = 6x10^{-4}$ m (micrometric cavity). The continuous line is the FlexPDE-model data. The dotted line is the Comsol Multiphysics model data.

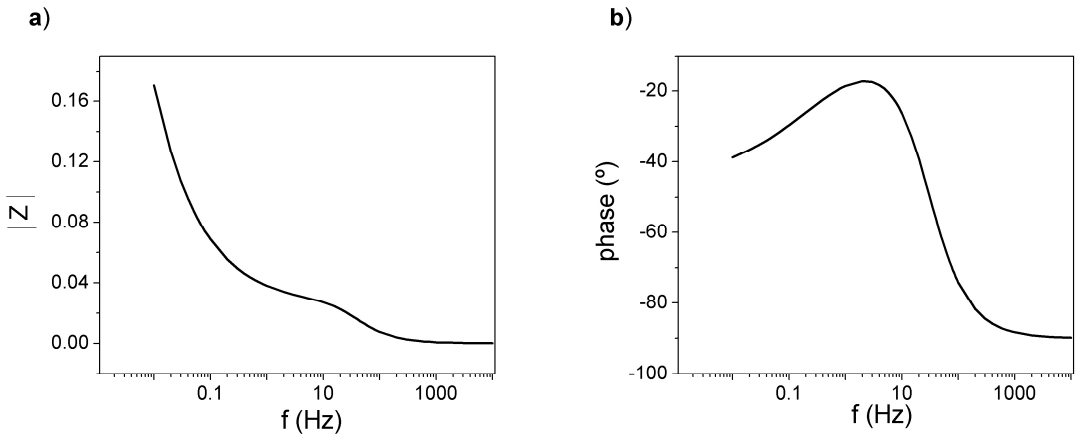

Figure 2. Bode plot of the modelled electrochemical reaction with $C^*_k = 1$ mol/m^3, $D_k = 1\text{x}10^{-10}$ m^2/s, $\alpha_c = 0.5$, $k^0 = 1\text{x}10^{-5}$ m/s, $C_{dl} = 0.2$ F/m^2, $n = 1$, $T = 298.15$ K, and d = 6x10^{-4} m (micrometric cavity): a) impedance magnitude, b) impedance phase.

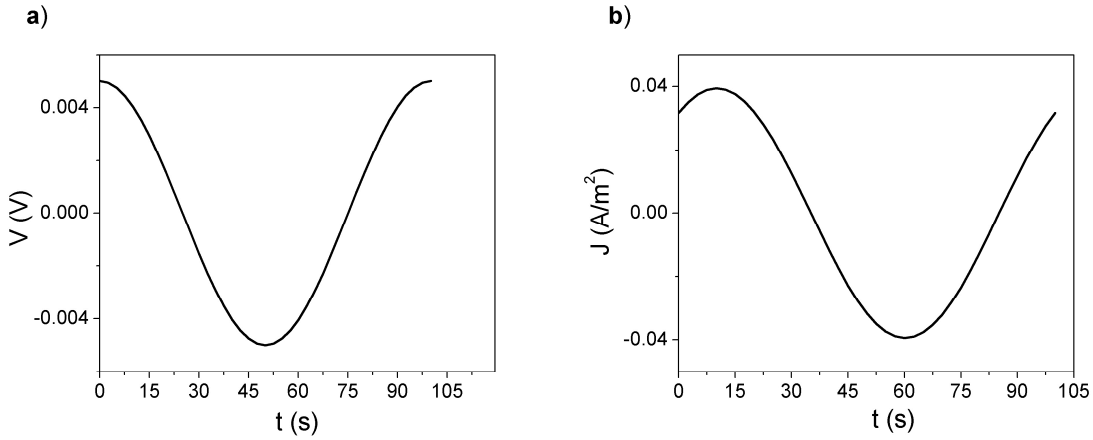

Figure 3. Recovered time profile of the complex signal for $f = 1\text{x}10^{-2}$ Hz: a) voltage, b) total current density. $C^*_k = 1$ mol/m^3, $D_k = 1\text{x}10^{-10}$ m^2/s, $\alpha_c = 0.5$, $k^0 = 1\text{x}10^{-5}$ m/s, $C_{dl} = 0.2$ F/m^2, $n = 1$, $T = 298.15$ K, and d = 6x10^{-4} m (micrometric cavity).

Figure 4 shows the real (Figure 4a) and imaginary (Figure 4b) components of the reacting-species complex-concentration through the electrolyte diffusion layer, for a frequency $f = 1\text{x}10^{-2}$ Hz (mass-transport-controlled region). The characteristic damped-oscillations can be observed. Thus, the complex concentration amplitude, calculated from both components, decreases towards the electrolyte bulk. It is by definition positive, so it is of none use to analyze the direction of species movement with respect to the voltage input signal. At the electrode surface ($x = 0$) the ratio imaginary-component/real-component leads to a phase shift of about -40° (which agrees with Figure 3). At that position, both reactive species have a negligible imaginary component, suggesting the concentration signal goes almost in-phase with the applied potential. The negative real-component of the A-species (reduced species, R_k) indicates then, the species is being consumed while the electrode sustains a positive overpotential. Such situation is the expected behavior at the lowest signal frequencies. The program seems to be then free of user-input errors and can be further modified to analyze more complicated impedance situations.

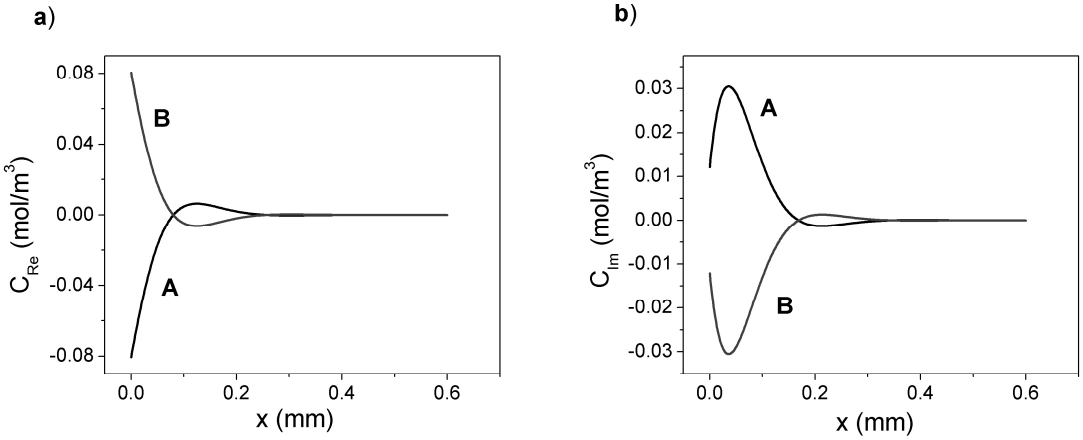

Figure 4. Real (a) and imaginary (b) components of the complex concentration of reacting species A and B, at a frequency $f = 1\text{x}10^{-2}$ Hz. $C^*_k = 1$ mol/m^3, $D_k = 1\text{x}10^{-10}$ m^2/s, $\alpha_c = 0.5$, $k^0 = 1\text{x}10^{-5}$ m/s, $C_{dl} = 0.2$ F/m^2, $n = 1$, $T = 298.15$ K, and $d = 6\text{x}10^{-4}$ m (micrometric cavity).

Conclusions

The development of electrochemical-impedance-spectroscopy computational-models is a swift way to accelerate the learning experience with such a complex technique. However, even simple models can result complicated due to the work with complex differential equations. The key to assess the model reliability is to exhaustively use graphical output resources to analyze the relation between frequency-domain signals and time-domain recovered profiles. Such information is very well contained within the amplitude and phase concepts. In principle, once the simple-model base is securely stablished, advanced elements can then be step-wise integrated to study their effect over the resulting impedance spectra. In this way, effects such as porosity and finite-length diffusion effects can be more readily identified and isolated from experimental spectra.

Acknowledgments

The authors gratefully acknowledge financial support from the “Direccion General de Asuntos del Personal Academico (DGAPA) de la Universidad Nacional Autonoma de Mexico”, project PAPIIT IA105218, and from the “Facultad de Quimica de la Universidad Nacional Autonoma de Mexico”, projects PAIP 5000-9150 and PAIP 5000-9087.

References

1. A. Lasia, *Electrochemical Impedance Spectroscopy and its Applications*, Springer Science + Business Media, New York (2014).

2. X.-Z. Yuan, C. Song, H. Wang and J. Zhang, *Electrochemical Impedance Spectroscopy in PEM Fuel Cells. Fundamentals and Applications*, Springer Verlag, London (2010).
3. *Impedance Spectroscopy Theory, Experiment, and Applications*, E. Barsoukov and J. R. Macdonald, Editors, John Wiley & Sons, New Jersey (2005).
4. R. V. Quevedo-Robles, G.A. Grijalva-Bustamante, T. del Castillo-Castro, M. M. Castillo-Ortega, D. E. Rodríguez-Félix, T. E. Lara, R. Mayen-Mondragon and I. Santos, *Synth. Met.*, **253**, 100 (2019).
5. O. J. Marquez-Calles, R. D. Martinez-Orozco, N. V. Gallardo-Rivas, A. M. Mendoza-Martinez, R. Mayen-Mondragon and U. Paramo-Garcia, *Int. J. Electrochem. Sci.,* **14** (6), 5200 (2019).
6. R. Mayen-Mondragon and J. Genesca-Llongueras, *ECS Trans.*, **76** (1), 53 (2017).
7. R. Mayen-Mondragon, R. Montoya-Lopez and J. Genesca-Llongueras, *ECS Trans.*, **84** (1), 131 (2018).
8. M.C. Quevedo, G. Galicia, R. Mayen-Mondragon and J. Genesca, *J. Mater. Res. Technol.*, **7** (2), 149 (2018).
9. A. J. Bard and L. R. Faulkner, *Electrochemical Methods. Fundamentals and Applications*, John Wiley & Sons, New York (2001).